

ACCEPTED MANUSCRIPT

Ultrathin-film optical coating for angle independent remote hydrogen sensing

To cite this article before publication: Mohamed ElKabbash *et al* 2020 *Meas. Sci. Technol.* in press <https://doi.org/10.1088/1361-6501/ab9fd8>

Manuscript version: Accepted Manuscript

Accepted Manuscript is “the version of the article accepted for publication including all changes made as a result of the peer review process, and which may also include the addition to the article by IOP Publishing of a header, an article ID, a cover sheet and/or an ‘Accepted Manuscript’ watermark, but excluding any other editing, typesetting or other changes made by IOP Publishing and/or its licensors”

This Accepted Manuscript is © 2020 IOP Publishing Ltd.

During the embargo period (the 12 month period from the publication of the Version of Record of this article), the Accepted Manuscript is fully protected by copyright and cannot be reused or reposted elsewhere.

As the Version of Record of this article is going to be / has been published on a subscription basis, this Accepted Manuscript is available for reuse under a CC BY-NC-ND 3.0 licence after the 12 month embargo period.

After the embargo period, everyone is permitted to use copy and redistribute this article for non-commercial purposes only, provided that they adhere to all the terms of the licence <https://creativecommons.org/licenses/by-nc-nd/3.0>

Although reasonable endeavours have been taken to obtain all necessary permissions from third parties to include their copyrighted content within this article, their full citation and copyright line may not be present in this Accepted Manuscript version. Before using any content from this article, please refer to the Version of Record on IOPscience once published for full citation and copyright details, as permissions will likely be required. All third party content is fully copyright protected, unless specifically stated otherwise in the figure caption in the Version of Record.

View the [article online](#) for updates and enhancements.

Ultrathin-film optical coating for angle independent remote hydrogen sensing

Mohamed ElKabbash^{1,2*}, Kandammathe Valiyaveedu Sreekanth¹, Arwa Fraiwan³, Jonathan Cole⁴, Yunus Alapan³, Theodore Letsou¹, Nathaniel Hoffman¹, Chunlei Guo², R. Mohan Sankaran⁴, Umut A. Gurkan^{3,5,6,7}, Michael Hinczewski¹, Giuseppe Strangi^{1,8,9*}

^{1.} Department of Physics, Case Western Reserve University, 10600 Euclid Avenue, Cleveland, Ohio 44106, USA.

^{2.} The Institute of Optics, University of Rochester, Rochester, NY 14627, USA.

^{3.} Case Biomanufacturing and Microfabrication Laboratory, Mechanical and Aerospace Engineering Department, Case Western Reserve University, Cleveland, Ohio 44106.

^{4.} Department of Chemical and Biomolecular Engineering, Case Western Reserve University, Cleveland, OH, USA.

^{5.} Biomedical Engineering Department, Case Western Reserve University, Cleveland, Ohio 44106, USA.

^{6.} Department of Orthopedics, Case Western Reserve University, Cleveland, Ohio 44106, USA.

^{7.} Advanced Platform Technology Center, Louis Stokes Cleveland Veterans Affairs Medical Center, Cleveland, Ohio 44106, USA.

^{8.} CNR-NANOTEC, Istituto di Nanotecnologia and Department of Physics, University of Calabria, Italy.

^{9.} Istituto Italiano di Tecnologia, Via Morego 30, 16163, Genova, Italy.

Email: mke23@case.edu, qxs284@case.edu.

Abstract

We demonstrate an optically active antireflection, light absorbing, optical coating as a hydrogen gas sensor. The optical coating consists of an ultrathin 20 nm thick palladium film on a 60 nm thick germanium layer. The ultrathin thickness of the Pd film (20 nm) mitigates mechanical deformation and leads to robust operation. The measurable quantities of the sensors are the shift in the reflection minimum and the change in the full width at half maximum of the reflection spectrum as a function of hydrogen gas concentration. At a hydrogen gas concentration of 4%, the reflection minimum shifted by ~46 nm and the FWHM increased by ~228 nm. The sensor showed excellent sensitivity demonstrating a 6.5 nm wavelength shift for 0.7% hydrogen concentration, which is a significant improvement over other nanophotonic hydrogen sensing methods. Although the sensor's response showed hysteresis after cycling hydrogen exposure, the sensor is robust and showed no deterioration in its optical response after hydrogen deintercalation.

Keywords: Anti-reflection coatings, Hydrogen sensing, Light absorbers, Thin-films.

1- Introduction

Optical coatings are present in almost every optical instrument, with widespread applications ranging in displays and lighting ^{1,2}, to anticounterfeiting ³, and photovoltaics ⁴. Recently, absorptive, anti-reflection optical coatings were developed where either transmission is not of importance, e.g., structural coloring ⁵, and realization of generalized Brewster angle effect ⁶, or where high absorption is desired, e.g., for heat-assisted magnetic recording ⁷, solar-thermal power generation ⁸, and radiative cooling ⁹.

Light absorption is realized in optical coatings when light is critically coupled to the resonator, i.e., the absorption rate is equal to the reflection and transmission rates. This occurs when the interfering waves are out of phase (phase condition), and the out-of-phase waves are of equal amplitude (amplitude condition) ^{10,11}. For ultrathin film optical coatings light absorbers, critical light coupling is typically achieved by two strategies; (1) using a lossy-dielectric on a highly reflective substrate ¹², e.g., Ag, Au, or Al, or (2) using a lossless dielectric on a low-reflectance substrate ¹³, e.g., Ni, Ti, or Pd. In addition, it has been shown that dielectrics with high refractive index lead to angle independent light absorption ¹¹. Angle independent light absorption leads to robust operation of optical coatings even on rough surfaces such as unpolished glass or paper ¹⁴.

On the other hand, hydrogen sensing is of crucial importance to industries where hydrogen gas (H_2) is present, e.g., in nuclear power stations, coal mines, lighting industry, and semiconductor manufacturing, etc., ¹¹. Hydrogen is flammable with low ignition energy at concentrations from 4% to 75% ¹⁵. Hydrogen sensors must be able to provide strong response to concentrations significantly lower than the explosive level of 4% to provide adequate warning before an explosion hazard takes place ¹⁶. Although there exist many well-established hydrogen sensing technologies by measuring, e.g., the change in resistance of Pd wires ¹⁷, photonic-based hydrogen sensing is especially attractive as it allows for remote optical interrogation where the raw signal is optical instead of electrical. Photonic hydrogen sensors avoid the risk of being a possible source of ignition if a hydrogen leaks occurs ¹⁸.

Several systems have been reported as a platform for optical hydrogen sensing ^{15,19}. In general, photonic-based hydrogen sensors measure changes in the refractive index of

1
2
3 materials that form hydrides , i.e., they are hydride-based refractometers ²⁰, most commonly
4 using palladium (Pd). When Pd is exposed to H₂, it forms palladium hydride, PdH_x, which has
5 a different complex refractive index than Pd that depends on the hydrogen stoichiometry ²¹.
6 At low H₂ concentrations, the intercalated hydrogen atoms are randomly situated inside the
7 Pd lattice, forming a solid solution (α phase) ²². At higher H₂ concentrations, the hydrogen
8 atoms are ordered in the lattice forming a hydride β phase ²³, which leads to an increase in
9 the lattice parameter by $\sim 3.5\%$ and an expansion of the Pd film. The resulting tensile stress
10 causes mechanical deformation and the formation of cracks can significantly degrade sensor
11 performance over time ¹⁶. The formation of hydrides leads to a decrease in the absolute value
12 of both the real and imaginary components of the complex refractive index of Pd ¹⁵. Changes
13 in Pd dielectric constant can be measured by directly measuring small changes in reflection
14 ⁶, or scattering of Pd nanoparticles ²⁴. In addition, formation of hydrides can be measured
15 indirectly by coating Pd on an optical fiber and measuring the changes in the output signal ²⁵
16 or measuring the scattering of a plasmonic nanoparticle that acts as a refractometer ²⁶. In the
17 context of thin Pd films, optical hydrogen sensing was demonstrated based on directly
18 measuring changes in reflection²⁰ or transmission²⁷ due to hydride formation.
19
20
21
22
23
24
25
26
27
28
29
30
31

32 In this work, we demonstrate a nanophotonic hydrogen sensor based on an antireflective
33 (absorptive) optical coating that suppresses light reflection in the telecommunication
34 wavelength range. The dielectric-metal antireflective absorptive coating consists of a Ge and
35 Pd ultrathin film. The ultrathin thickness of Pd mitigates mechanical deformation in Pd-
36 based hydrogen sensors by reducing the clamping effect ²⁸. The Pd film forms a Pd hydride
37 upon exposure to hydrogen which alters the wavelength of minimum reflection, λ_{min} , and
38 the full width at half maximum (FWHM) of the light absorber. The measured shift in λ_{min} is
39 ~ 46 nm at the critical H₂ concentration of 4%, which is significantly higher than other
40 nanophotonic gas sensors ^{15,19}. Due to the high refractive index of Ge, λ_{min} is angle
41 independent over a wide range of angles ($25^\circ - 45^\circ$), and the shift in λ_{min} is approximately
42 the same for all the measured incident angles. We show that the change in FWHM is an
43 important sensing parameter reaching up to 228 ± 4 nm at 45° . The demonstrated sensor is
44 inexpensive and can be deposited over a large area which enables scalable hydrogen
45 monitoring ²⁰.
46
47
48
49
50
51
52
53
54
55
56
57
58
59
60

2- Experimental:

2.1- Sensor fabrication:

The sensor consists of a 20 nm thick Pd film on top of a 60 nm thick Ge layer, each deposited by electron beam evaporation at a rate of $0.5 \text{ \AA} \cdot \text{s}^{-1}$ on a 1 mm thick glass slide (see **Fig. 1a**). The Pd thickness was chosen to be ~ 20 nm to mitigate mechanical deformation by the clamping effect where the tensile stiffness of a film is inversely proportional to its thickness¹⁵. We chose Ge to serve as a dielectric as it has a high refractive index in the near infrared NIR region with negligible optical losses²⁹. As we showed previously, a high index dielectric results in angle independent light absorption in thin-film absorbers¹⁴. The Ge thickness was chosen to obtain a reflection minimum within the telecom wavelength windows (~ 1300 nm-1600 nm). To expose the sensor to hydrogen, we fabricated a microfluidic channel on the sensor (see **Fig. 1a**). The channel consists of a poly (methyl methacrylate) (PMMA) body (encompassing laser micromachined inlets and outlets) and a double-sided 100- μm adhesive film defining the outlines and thickness of the microchannel. The microfluidic channel was attached to the Pd side and the reflection was interrogated from the glass side.

2.2- Experimental setup:

The sensor was placed on a variable angle ellipsometer (J. A. Woollam) to measure the angular reflectance R (**Fig. 1b**). To control the hydrogen concentration, a 4% hydrogen (H_2) in nitrogen (N_2) mixture was diluted by pure N_2 . The ratio of the two was varied by two digital mass flow controllers (MFCs) to obtain a final concentration between 0.7 and 4%. The reflection before introducing the hydrogen was measured and recorded. It is important to note that using an ellipsometer is ideal to perform angular reflectance measurement over a wide wavelength range, however, it limits our ability to determine the exact response time of the sensor. In all cases, the response time of a hydrogen sensor depends on the hydrogen diffusion coefficient in the active material, here Pd, and the film thickness³⁰. For the purpose of our experiments, we recorded the reflection after ~ 12 minutes from introducing the H_2/N_2 mixture to ensure that we observe the steady state reflection.

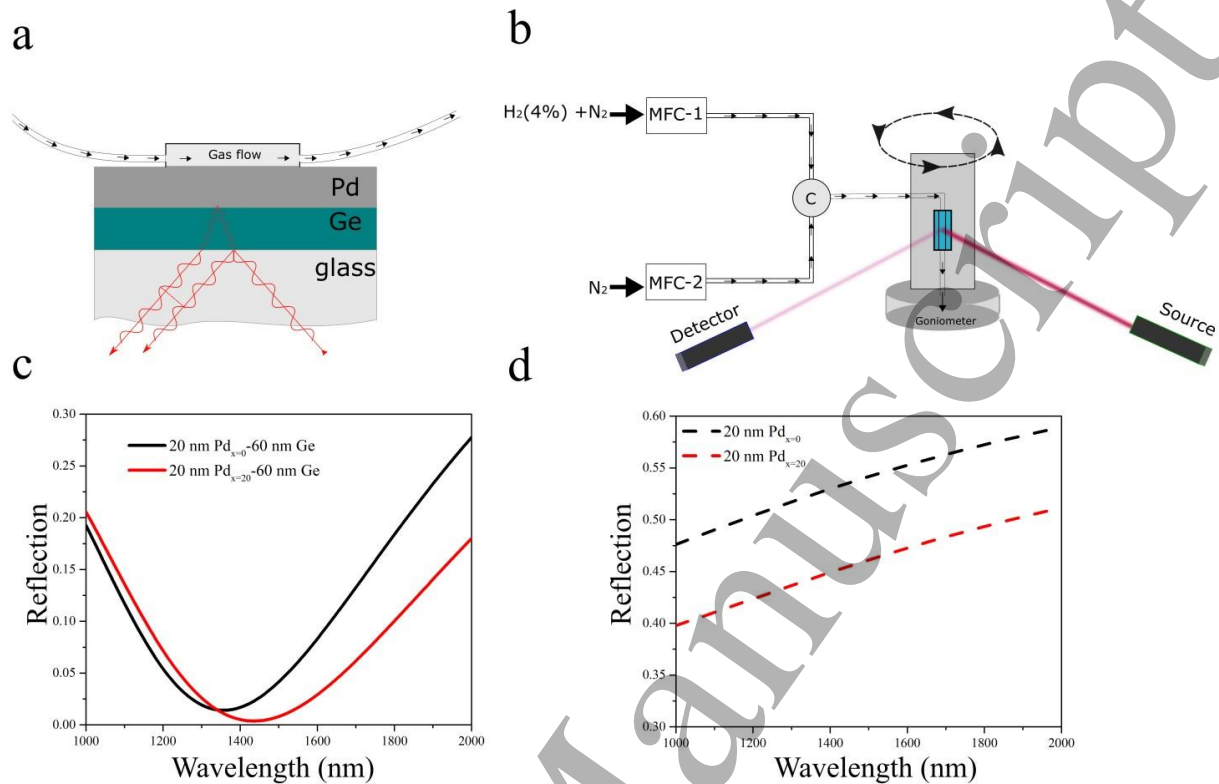


Fig. 1. : (a) A schematic of the optical coating sensor. The microfluidic channel is attached to the top of the Pd film to expose Pd to hydrogen. (b) The microfluidic channel is connected to two mass flow controllers (MFCs). One MFC controls the flow of nitrogen mixed with hydrogen (4% in concentration) and another MFC controls the flow of pure nitrogen. The sensor is placed on a variable angle ellipsometer to measure the angular reflectivity. Calculated reflectance of (c) Pd-Ge optical coating and (d) a Pd film, for hydrogen atomic ratio $x=0$ (black line), $x = 20\%$ (red line).

3- Theoretical background:

To understand the sensing mechanism, we investigate how the optical properties of our absorber depend on wavelength. The system of interest can be defined as a glass substrate with a refractive index n_0 (glass), a lossless dielectric layer with thickness h and refractive index n_D (Ge), and a lossy substrate with refractive index $n_s + ik_s$ (Pd). Light is incident on the system with wavelength, λ , and incident angle, θ . Following the theory described in ¹⁴, we can express the conditions for perfect absorption as:

$$\tan \phi_D = \frac{(n_S - \gamma_0)\gamma_D}{k_S\gamma_0} = \frac{k_S\gamma_D}{\gamma_D^2 - n_S\gamma_0} \quad (1)$$

where $\gamma_0 = n_0/\cos \theta$, $\gamma_D = n_D^2/\sqrt{n_D^2 - n_0^2\sin^2\theta}$, and $\phi_D = 2\pi hn_D^2/(\lambda\gamma_D)$. The latter is the phase gain in one pass through the dielectric layer. Note that to derive the above expressions, we assumed $|n_0 \sin \theta / (n_S + ik_S)|^2 \ll 1$, which is valid for the system under consideration. Both equalities in the equation above must be simultaneously satisfied for perfect absorption to occur. In the simplest scenario, we can ignore the dependence of n_0 and n_D on λ , so that we can rewrite the conditions for perfect light absorption directly in terms of λ_{min} :

$$\lambda_{min} = \frac{2\pi hn_D^2}{\gamma_D \left[m\pi + \tan^{-1} \left(\frac{(n_S - \gamma_0)\gamma_D}{k_S\gamma_0} \right) \right]} \quad (2)$$

where m is an integer. Equation (2) shows that as n_S and k_S vary, the value of λ_{min} where perfect absorption takes place will also shift. Even if the variation in n_S and k_S does not perfectly preserve in Eq. (2), the equation still serves as an approximation for how λ_{min} changes. Clearly, changes in n_S and k_S of the metallic substrate can lead to a strong shift in λ_{min} . In addition, for a thin-film light absorber, the absorption linewidth depends on the reflectance from each interface where broader absorption modes are obtained for metallic films with lower reflectance³¹. To confirm our expectations, we performed transfer matrix method calculation to calculate the reflection of the proposed Pd-Ge optical coating for hydrogen atomic ratio $x=0$ and 20% (**Fig. 1c**). The calculated shift in reflection minimum λ_{min} is 90 nm and the full width at half maximum has increased by ~ 200 nm. Conversely, the traditional direct measurement of the change in reflection of a Pd film, monitored from the glass slide, would lead to $\sim 8\%$ change in reflection as shown in **Fig. 1d**. The incident light is p-polarized for all the calculations and measurements presented in this manuscript. We note here that the thin film interference-based hydrogen sensing differs from hydrogen sensing by coating Pd or other chemochromic oxides coated onto the tip or along the length of an optical fiber that is later detected by means of interferometry³¹. In the latter case, Pd coats a small portion of the fiber and upon hydrogen exposure and lattice expansion, the fiber's effective optical path length changes¹⁵.

4- Result and discussion

Fig. 2a shows the measured reflection spectrum of the optical coating over the wavelength range 1000-2000 nm at 25° (top panel), 35° (middle panel), and 45° (bottom panel). We first note that λ_{min} occurs at similar wavelengths regardless of the incident angle. After introducing H₂ at 4% concentration, we see a clear shift in λ_{min} . The total shifts in λ_{min} are $46 \pm 2nm$, $47 \pm 2nm$, and $45 \pm 2nm$, at 25°, 35°, and 45°, respectively. The angle-independent sensitivity is an interesting property of the demonstrated sensor.

Fig. 2b and **2c** show contour maps of the angular reflectance for our sensors exposed to N₂ only and to H₂ (4% in N₂), respectively. In addition to the wavelength shifts, the FWHMs of the absorption modes significantly increase in the presence of H₂. The changes in the FWHM are $195 \pm 4nm$, $186 \pm 4nm$, and $228 \pm 4nm$, at 25°, 35°, and 45° respectively. The change in the FWHM can be measured by monitoring changes in the reflection intensity of a broadband NIR light source, e.g., using Tungsten Halogen and Krypton lamps. Sensors that rely on changes in the intensity may offer a cheaper alternative as they do not require using a spectrometer. For a broadband detector, the reflected power can be calculated as

$$P = \int \frac{h c}{\lambda} R(\lambda) d\lambda \quad (3)$$

where h and c are the Planck's constant and speed of light and $R(\lambda)$ is the spectral reflection of the sample. We can then calculate the percent power difference before and after introducing the hydrogen as follows:

$$\Delta P = \frac{P_{N_2} - P_{H_2}}{P_{H_2}} \times 100 \quad (4)$$

Where P_{N_2} and P_{H_2} are the reflected power from the sensor before and after introducing hydrogen, respectively. The increase in the FWHM due to introducing hydrogen is tantamount to a decrease in the total reflected power. The calculated ΔP is $\sim 25\%$, 28% , and

33% for a hydrogen concentration of 4% and an incident angle of 25°, 35°, and 45°, respectively.

We note that the change in the FWHM of the optical coating hydrogen sensor is an additional advantage over Fabry-Perot cavity hydrogen sensor which shows small overall change in the FWHM¹⁵. Furthermore, Fabry-Perot hydrogen sensors rely on cavity resonances which requires a dielectric with an optical thickness of at least $\lambda/2$ which requires excessively thick dielectric films when operating at longer wavelengths.

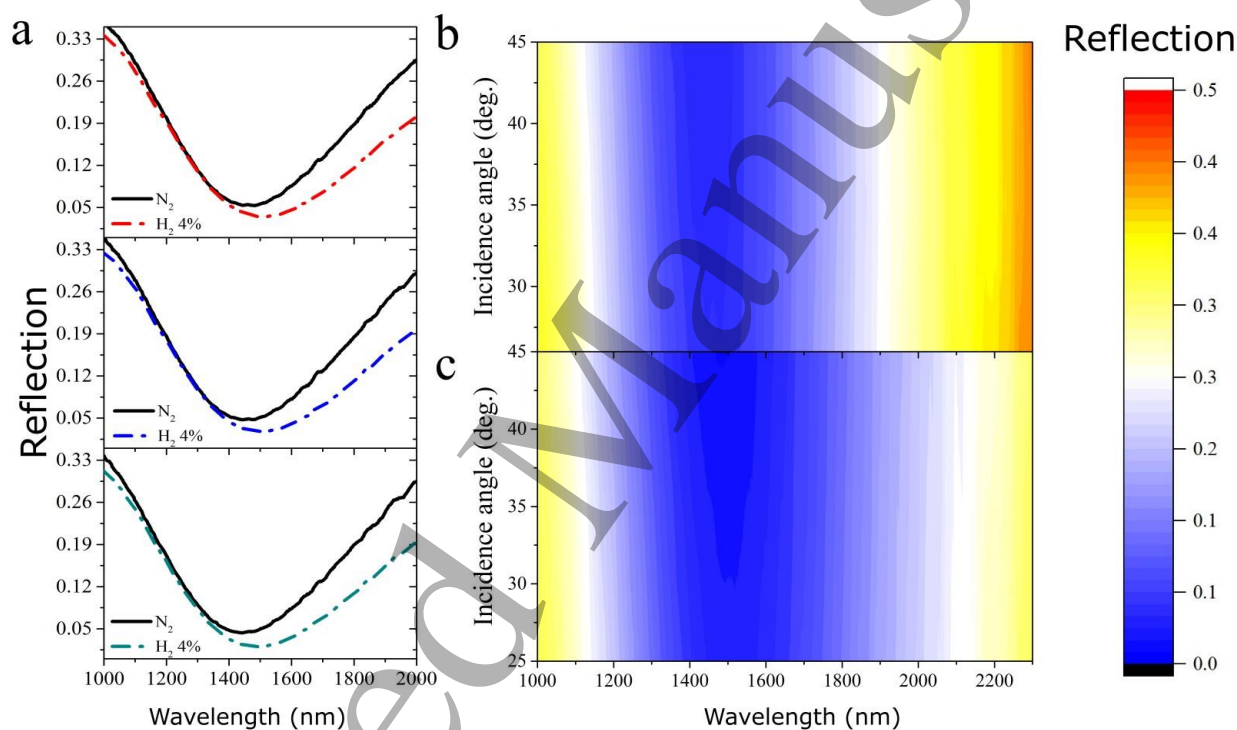


Fig. 2. (a) Reflection measurements for the optical absorber before and after introducing hydrogen with $C = 4\%$ for three different incident angles 25°, 35°, and 45°. A contour plot of the angular reflection shows the angular reflection of the absorber for (b) $C = 0\%$ and (c) $C = 4\%$. The FWHM increases significantly after introducing hydrogen for all incident angles.

Fig. 3a shows the shift in reflection at an incidence angle of 45° as a function of hydrogen concentration. We obtained shifts of 6.5 nm, 18.6 nm, and 44 nm at concentrations of 0.7%, 2%, and 4%, respectively. We note that the lowest hydrogen concentration used was determined based on the MFC control range and do not represent the lowest concentration that can be detected. For comparison, previous works showed ultrasensitive optical

1
2
3 hydrogen sensing with ~ 2.5 nm shift in wavelength for 0.6% hydrogen concentration³². In
4 our work, we demonstrate 6.5 nm shift for 0.7%.
5
6

7 We also studied the hysteresis behavior of the sensor. In general, when Pd forms a hydride,
8 a mechanical energy barrier is created due to the coherency strain produced by the lattice
9 expansion of the hydride phase⁶. This barrier prevents the release of hydrogen atoms
10 situated inside the hydride lattice to recover the original Pd structure. **Fig. 3b** shows a
11 hysteresis plot for the shift in λ_{min} at different H₂ concentrations (0%, 0.7%, 2% and 4%)
12 and 45° incidence angles. Each measurement presented is extracted from the steady state
13 reflection spectrum which was obtained after ~ 12 minutes for each concentration. The λ_{min}
14 is found to be higher when the H₂ concentration is decreased than when the H₂ concentration
15 is increased. We suggest that the hydrogen content or stoichiometries in terms of x in the
16 PdH_x are different during the forward and reverse cycles of exposing to different H₂
17 concentrations, with the stoichiometry being higher in the reverse cycle because of the
18 aforementioned mechanical energy barrier to deintercalation from coherency strain. We
19 note here that heating the sensor to higher temperatures could limit or eliminate the
20 observed hysteresis, however, on the expense of minimizing the sensitivity^{33,34}. Moreover,
21 using Pd alloys was shown to minimize the hysteresis significantly, e.g., using Pd Au
22 alloys^{35,36}. The existence of coherency strain, however, did not affect the overall performance
23 of our sensor as the absorption mode relaxed to the initial λ_{min} when the H₂ concentration
24 was decreased to zero (pure N₂).
25
26
27
28
29
30
31
32
33
34
35
36
37
38
39
40
41
42
43
44
45
46
47
48
49
50
51
52
53
54
55
56
57
58
59
60

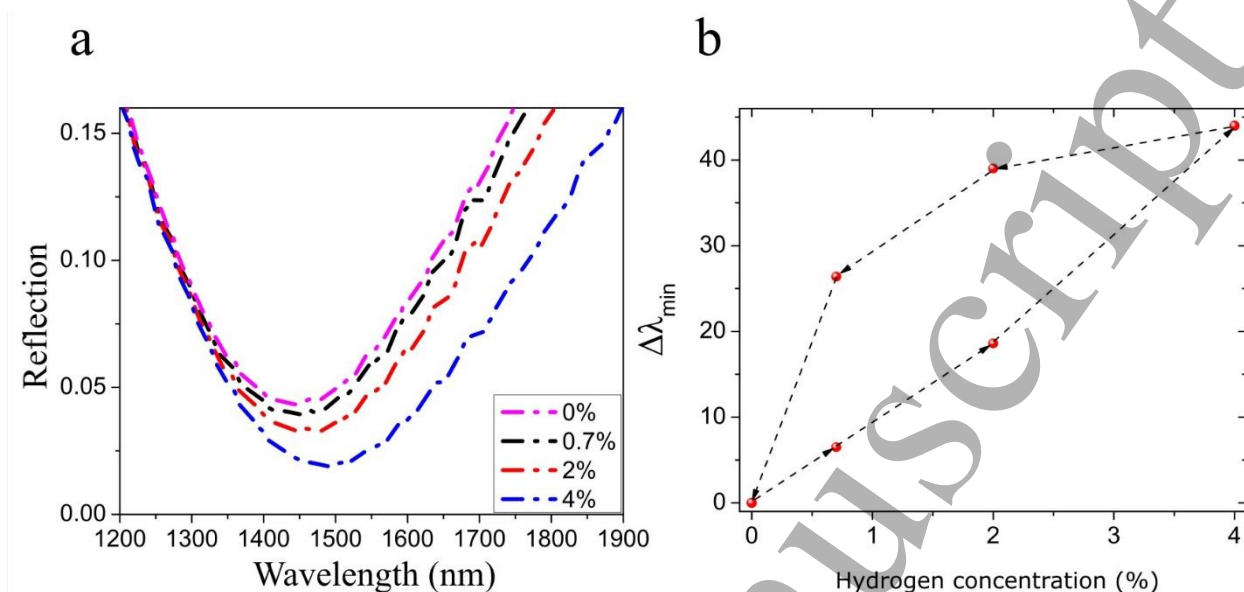


Fig. 3. (a) Reflection of the absorber as a function of hydrogen concentration. (b) Sensor response to hydrogen concentrations (0.7% - 4%) showing hysteresis behavior in reflectivity minimum, λ_{min} .

5- Conclusion

In summary, we developed an ultrathin film optical coating for hydrogen sensing. The sensor consists of an antireflective, absorptive Pd film. The change in the antireflection properties in terms of reflection minimum and FWHM enabled the detection of low hydrogen concentrations. The sensor shows similar overall shift in reflection minimum over a broad range of incidence angles. Hysteresis in the reflection minimum was found arising from a mechanical energy barrier to deintercalation but did not lead to degradation in the sensor performance. The hysteresis issue can be potentially mitigated by employing different types of Pd alloys as substrates. Moreover, using Pd alloys with higher hydrogen diffusion coefficients or using a substrate consisting of Pd nanowire mesh³⁷ can provide a sensor with a short response time.

Acknowledgements

G.S. received funding from the Ohio Third Frontier Project "Research Cluster on Surfaces in Advanced Materials (RCSAM) at Case Western Reserve University" and the GU Malignancies Program of the Case Comprehensive Cancer Centre and was supported in part by the National Science Foundation, Grant No. DMR-1708742. U.A.G. acknowledges National Heart

Lung and Blood Institute R01HL133574, and National Science Foundation CAREER Award #1552782. This article's contents are solely the responsibility of the authors and do not necessarily represent the official views of the National Institutes of Health.

Disclosures

The authors declare no conflicts of interest.

References

- 1 Macleod, H. A. *Thin film Optical Filters*. 4th edition edn, (London Adam Hilger, 1986).
- 2 L. E. Tannas, J. Flat-panel displays displace large, heavy, power-hungry CRTs. *IEEE Spectr.* **26**, 34-35, doi:10.1109/6.90181 (1989).
- 3 Hornbeck, L. J. *Digital Light Processing for high-brightness high-resolution applications*. Vol. 3013 EI (SPIE, 1997).
- 4 Dobrowolski, J. A., Ho, F. C. & Waldorf, A. Research on thin film anticounterfeiting coatings at the National Research Council of Canada. *Appl. Opt.* **28**, 2702-2717, doi:10.1364/AO.28.002702 (1989).
- 5 Chen, D. Anti-reflection (AR) coatings made by sol-gel processes: A review. *Solar Energy Materials and Solar Cells* **68**, 313-336, doi:[https://doi.org/10.1016/S0927-0248\(00\)00365-2](https://doi.org/10.1016/S0927-0248(00)00365-2) (2001).
- 6 Letsou, T., ElKabbash, M., Iram, S., Hinczewski, M. & Strangi, G. Heat-induced perfect light absorption in thin-film metasurfaces for structural coloring [Invited]. *Opt. Mater. Express* **9**, 1386-1393, doi:10.1364/OME.9.001386 (2019).
- 7 Sreekanth, K. V. *et al.* Generalized Brewster Angle Effect in Thin-Film Optical Absorbers and Its Application for Graphene Hydrogen Sensing. *ACS Photonics*, doi:10.1021/acsp Photonics.9b00564 (2019).
- 8 Deng, C. *et al.* Nanocavity induced light concentration for energy efficient heat assisted magnetic recording media. *Nano Energy* **50**, 750-755, doi:<https://doi.org/10.1016/j.nanoen.2018.06.036> (2018).
- 9 ElKabbash, M. *et al.* Tunable Black Gold: Controlling the Near-Field Coupling of Immobilized Au Nanoparticles Embedded in Mesoporous Silica Capsules. *Advanced Optical Materials* **5**, 1700617, doi:10.1002/adom.201700617 (2017).
- 10 Raman, A. P., Anoma, M. A., Zhu, L., Rephaeli, E. & Fan, S. Passive radiative cooling below ambient air temperature under direct sunlight. *Nature* **515**, 540, doi:10.1038/nature13883 (2014).
- 11 ElKabbash, M., Iram, S., Letsou, T., Hinczewski, M. & Strangi, G. Designer Perfect Light Absorption Using Ultrathin Lossless Dielectrics on Absorptive Substrates. *Advanced Optical Materials* **6**, 1800672, doi:10.1002/adom.201800672 (2018).
- 12 Kats, M. A. & Capasso, F. Optical absorbers based on strong interference in ultra-thin films. *Laser & Photonics Reviews* **10**, 735-749, doi:10.1002/lpor.201600098 (2016).
- 13 Kats, M. A., Blanchard, R., Genevet, P. & Capasso, F. Nanometre optical coatings based on strong interference effects in highly absorbing media. *Nature Materials* **12**, 20, doi:10.1038/nmat3443 <https://www.nature.com/articles/nmat3443#supplementary-information> (2012).
- 14 ElKabbash, M. *et al.* Iridescence-free and narrowband perfect light absorption in critically coupled metal high-index dielectric cavities. *Opt. Lett.* **42**, 3598-3601, doi:10.1364/OL.42.003598 (2017).
- 15 Hübert, T., Boon-Brett, L., Black, G. & Banach, U. Hydrogen sensors - A review. *Sensors and Actuators B: Chemical* **157**, 329-352, doi:<https://doi.org/10.1016/j.snb.2011.04.070> (2011).
- 16 Fong, N. R., Berini, P. & Tait, R. N. Hydrogen sensing with Pd-coated long-range surface plasmon membrane waveguides. *Nanoscale* **8**, 4284-4290, doi:10.1039/C5NR08001K (2016).
- 17 R. Pitts, P. L., S-H. Lee, E. Tracy. Interfacial Stability of Thin Film Hydrogen Sensors. *proceedings of the 2001 DOE hydrogen program review* (2001).
- 18 Sun, Y. & Wang, H. H. High-Performance, Flexible Hydrogen Sensors That Use Carbon Nanotubes Decorated with Palladium Nanoparticles. *Advanced Materials* **19**, 2818-2823, doi:10.1002/adma.200602975 (2007).
- 19 Tittel, A. *et al.* Palladium-Based Plasmonic Perfect Absorber in the Visible Wavelength Range and Its Application to Hydrogen Sensing. *Nano Letters* **11**, 4366-4369, doi:10.1021/nl202489g (2011).
- 20 Liu, N., Tang, M. L., Hentschel, M., Giessen, H. & Alivisatos, A. P. Nanoantenna-enhanced gas sensing in a single tailored nanofocus. *Nature Materials* **10**, 631, doi:10.1038/nmat3029 (2011).
- 21 Sreekanth, K. V. *et al.* Hyperbolic metamaterials-based plasmonic biosensor for fluid biopsy with single molecule sensitivity. *EPJ Applied Metamaterials* **4**, 1 (2017).
- 22 Vargas, W. E., Rojas, I., Azofeifa, D. E. & Clark, N. Optical and electrical properties of hydrided palladium thin films studied by an inversion approach from transmittance measurements. *Thin Solid Films* **496**, 189-196, doi:<https://doi.org/10.1016/j.tsf.2005.08.346> (2006).

- 1
2
3 23 Syrenova, S. *et al.* Hydride formation thermodynamics and hysteresis in individual Pd nanocrystals with different
4 size and shape. *Nature Materials* **14**, 1236, doi:10.1038/nmat4409
5 <https://www.nature.com/articles/nmat4409#supplementary-information> (2015).
- 6 24 Cheng, Y.-T., Li, Y., Lisi, D. & Wang, W. M. Preparation and characterization of Pd/Ni thin films for hydrogen sensing.
7 *Sensors and Actuators B: Chemical* **30**, 11-16, doi:[https://doi.org/10.1016/0925-4005\(95\)01734-D](https://doi.org/10.1016/0925-4005(95)01734-D) (1996).
- 8 25 Wadell, C., Syrenova, S. & Langhammer, C. Plasmonic Hydrogen Sensing with Nanostructured Metal Hydrides. *ACS*
9 *Nano* **8**, 11925-11940, doi:10.1021/nn505804f (2014).
- 10 26 Zhang, Y.-n. *et al.* Recent advancements in optical fiber hydrogen sensors. *Sensors and Actuators B: Chemical* **244**,
11 393-416, doi:<https://doi.org/10.1016/j.snb.2017.01.004> (2017).
- 12 27 Zhao, Z., Carpenter, M., Xia, H. & Welch, D. All-optical hydrogen sensor based on a high alloy content palladium
13 thin film. *Sensors and Actuators B: Chemical* **113**, 532-538 (2006).
- 14 28 Cheong, H., Young Shim, J., Dong Lee, J., Mo Jin, J. & Lee, S.-H. Comparison of Pd, Pt and Pt/Pd as catalysts for
15 hydrogen sensor films. *Journal of Korean Physical Society* **55**, 2693 (2009).
- 16 29 Lee, E., Lee, J. M., Koo, J. H., Lee, W. & Lee, T. Hysteresis behavior of electrical resistance in Pd thin films during the
17 process of absorption and desorption of hydrogen gas. *International Journal of Hydrogen Energy* **35**, 6984-6991,
18 doi:<https://doi.org/10.1016/j.ijhydene.2010.04.051> (2010).
- 19 30 Liu, Y., Li, Y., Huang, P., Song, H. & Zhang, G. Modeling of hydrogen atom diffusion and response behavior of
20 hydrogen sensors in Pd-Y alloy nanofilm. *Scientific Reports* **6**, 37043, doi:10.1038/srep37043 (2016).
- 21 31 Li, Z., Butun, S. & Aydin, K. Large-Area, Lithography-Free Super Absorbers and Color Filters at Visible Frequencies
22 Using Ultrathin Metallic Films. *ACS Photonics* **2**, 183-188, doi:10.1021/ph500410u (2015).
- 23 32 Jiang, R., Qin, F., Ruan, Q., Wang, J. & Jin, C. Ultrasensitive Plasmonic Response of Bimetallic Au/Pd Nanostructures
24 to Hydrogen. *Advanced Functional Materials* **24**, 7328-7337, doi:10.1002/adfm.201402091 (2014).
- 25 33 Lewis, F. Palladium-hydrogen system. *Platinum Metals Review* **38**, 112-118 (1994).
- 26 34 Fisser, M., Badcock, R. A., Teal, P. D. & Hunze, A. Optimizing the sensitivity of palladium based hydrogen sensors.
27 *Sensors and Actuators B: Chemical* **259**, 10-19, doi:<https://doi.org/10.1016/j.snb.2017.11.180> (2018).
- 28 35 Bannenberg, L. J. *et al.* Direct Comparison of PdAu Alloy Thin Films and Nanoparticles upon Hydrogen Exposure.
29 *ACS applied materials & interfaces* **11**, 15489-15497 (2019).
- 30 36 Luo, S., Wang, D. & Flanagan, T. B. Thermodynamics of hydrogen in fcc Pd- Au alloys. *The Journal of Physical*
31 *Chemistry B* **114**, 6117-6125 (2010).
- 32 37 Zeng, X. Q. *et al.* Hydrogen Gas Sensing with Networks of Ultrasmall Palladium Nanowires Formed on Filtration
33 Membranes. *Nano Letters* **11**, 262-268, doi:10.1021/nl103682s (2011).
- 34
35
36
37
38
39
40
41
42
43
44
45
46
47
48
49
50
51
52
53
54
55
56
57
58
59
60